Title

Water contact angles on quartz surfaces under supercritical CO2 sequestration conditions: Experimental and molecular dynamics simulation studies

Authors

Chen, Cong
Wan, Jiamin
Li, Weizhong
et al.

Publication Date

2015-11-01

DOI

10.1016/j.ijggc.2015.09.019

Peer reviewed

Water contact angles on quartz surfaces under supercritical CO_2 sequestration conditions: Experimental and molecular dynamics simulation studies

Author links open overlay panel CongChen[a] JiaminWan[b] WeizhongLi[a] YongchenSong[a]
Show more

https://doi.org/10.1016/j.ijggc.2015.09.019 Get rights and content

Highlights

- Water contact angles on quartz surface linearly increases as ionic strength increases and the pressure and temperature have insignificant effects.
- The predicted water contact angles using molecular dynamics simulation methods agree well with those measured by experiments.
- CO_2 molecules adsorbed on a flat quartz surface can be easily replaced by water molecules and have no lasting effects on contact angles.

Abstract

The ambiguity of contact angle experimental measurements due to surface chemistry changes resulted from sample contamination and/or the degrees of reaction with supercritical CO_2 has resulted in great difficulties to precisely understand the wetting behavior of CO_2 under the geological carbon sequestration (GCS) conditions. In this study, water contact angles on quartz surface under GCS conditions were investigated through the combined experimental and molecular dynamics simulation (MDS) methods. The experimental results show that water contact angles increases as ionic strength increases. The effects of pressure and temperature are very weak. The dependence of ionic strength, pressure and temperature is same for monovalent and divalent ions solutions. In the MDS, a hydroxylated quartz surface was used as the base point. A good agreement between the MDS and experimental results were obtained. Using the MDS method, a clean mineral surface with a desired surface chemistry can be constructed, which is difficult in experiments. So by comparing MDS and experimental results, the mechanisms of the reservoir wettability can be better understood. Further investigation can be made on quartz surface with different

functional groups to better understand wettability alteration caused by contamination and/or CO_2 reaction.

Graphical abstract

Water contact angles as a function of ionic strength.

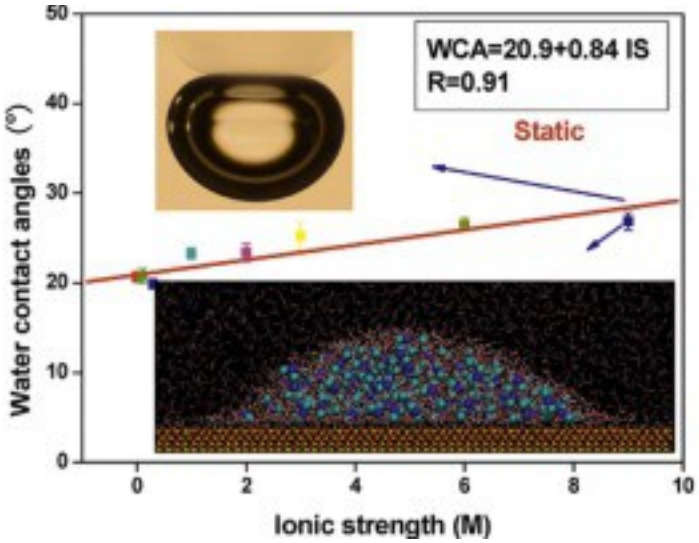

1. Download high-res image (189KB)
2. Download full-size image

- **Previous** article in issue
- **Next** article in issue

Keywords

Contact angle
Molecular dynamics simulation
Supercritical CO_2
Quartz
Wettability
Geological carbon sequestration

1. Introduction

CO_2 sequestration in deep saline aquifers has been regarded as one promising strategy to reverse the trend of increasing CO_2 emissions to the atmosphere (Altman et al., 2014). Interfacial characteristics such as interfacial tension and wettability among supercritical CO_2, brine and rock have a strong effect on capillary pressure, relative permeability and the behavior of phases (Michael et al., 2010, Song and Zhang,

2013, Tokunaga and Wan, 2013). When injecting supercritical CO_2 into saline aquifers, rock wettability among CO_2 and brine is a key factor which must be understood. Wettability of CO_2/water/solid systems has been extensively studied by experiments (Iglauer et al., 2015). A novel high-pressure apparatus has been developed to measure CO_2/water/solid contact angles for pressure up to 20.4 MPa (Dickson et al., 2006). They found contact angles increased significantly with CO_2 pressure for glasses with different hydrophilicities. During a comparison study between mica and quartz, a transition from strong water-wet to intermediate water-wet was captured during increasing pressures and the changing of wettability was more pronounced in the case of mica (Chiquet et al., 2007). Water contact angles on glass surfaces against dense CO_2 at 313 K as a function of pressure were investigated (Sutjiadi-Sia et al., 2008). It has been concluded that contact angles increased with increasing pressure in the gaseous region. However, in supercritical regime, contact angles showed little dependence on CO_2 pressure. Contact angles of the reservoir brine–reservoir rock system with dissolution of CO_2 at high pressure and elevated temperature were determined (Yang et al., 2008). According to their results, equilibrium contact angle increased as pressure increased, whereas it decreased as temperature increased. A pressurized glass micromodel was used to investigate wettability and they did not find transition from a water-wet system to an intermediate-wet system while increasing pressure up to 10 MPa (Chalbaud et al., 2009). It has been found that contact angles varied with CO_2 pressure (Espinoza and Santamarina, 2010): it increased on non-wetting surfaces such as PTEE and oil-wet quartz and slightly decreased in water-wet quartz and calcite surfaces. By repeatedly exposing samples to dense, water saturated CO_2, a permanent shift in contact angles has been found (Bikkina, 2011). However, the results were doubted and discussed in communications (Bikkina, 2012, Mahadevan, 2012). Silica wettability in CO_2–brine systems under pressure from 0.1 to 25 MPa and ionic strength from 0 to 5.0 M was studied (Jung and Wan, 2012). They found that water contact angles increased as pressure increased at moderate pressures from 7 to 10 MPa and remained nearly constant at pressure greater than 10 MPa. Within ionic strengths they selected, water contact angles increased nearly linearly with ionic strength. Pore-scale wettability and wettability alteration in CO_2–brine–silica systems were investigated using micromodels and dewetting of silica surfaces has been found where water contact angles increased from 0° up to 80° with large increases under higher ionic strength (Kim et al., 2012). A set of contact angles for CO_2/water/rock systems were reported (Farokhpoor et al., 2013). According to their data, quartz and calcite were strongly water wet and water contact angles nearly did not change with pressure, however, wettability of mica

changed from strongly water-wet to intermediate water-wet as pressure increased. An increasing of water contact angles as CO_2 pressure and temperature increased were found (Saraji et al., 2013). The pressure change occurred mostly in phase transition zone and as pressure increased further, water contact angles remained unchanged. Contact angles for several solids under CO_2 sequestration conditions have been studied and the results showed that pressure and temperature affected contact angles little, however, pH value and ionic strength can give larger contact angle changing (Wang et al., 2013a). Later, they investigated CO_2 adhesion on hydrated mineral surfaces and for dynamic contact angles, adhesion increased the angle by two times (Wang et al., 2013b). Pore scale contact angle measurements at reservoir conditions were conducted using X-ray micro-tomography (Andrew et al., 2014) and they observed that CO_2–brine–carbonate system was weakly water-wet with contact angles ranging from 35° to 55°. Wettability of a CO_2/water/Bentheimer sandstone system was evaluated and the effects of saturation degree, bubble size, surface roughness and pressure were analyzed (Kaveh et al., 2014). They found that phase transition of CO_2 from subcritical to supercritical had no effect on water contact angles for Bentheimer sandstone. The effects of surfactant on wettability were investigated and it has been found that by adding a surfactant, the contact angle in CO_2–water–SiO_2 system increased from 20 °C at 0.1 MPa to 70 °C at 10 MPa (Kim and Santamarina, 2014). Dynamic contact angles of CO_2/brine/quartz systems were investigated (Saraji et al., 2014). According to their results, the dynamic contact angles did not change significantly with pressure, however, they increased as brine salinity increased. Influence of temperature and pressure on quartz–water–CO_2 contact angles was investigated (Sarmadivaleh et al., 2015) and significant increase of contact angles with pressure and temperature increasing was observed. Water contact angles under N_2/CO_2mixture atmosphere on quartz at CO_2 storage site conditions in Gippsland basin were studied (Al-Yaseri et al., 2015a). The effects of pressure, temperature, surface roughness, salt type and brine salinities on dynamic contact angles were also investigated (Al-Yaseri et al., 2015b).

The above work mentioned as well as those cited in these literature have greatly improved our understanding of wettability of CO_2–brine–mineral systems under sequestration conditions. However, the reported contact angles varied significantly for similar conditions, and were even inconsistent in their trends with respect to changes in pressure and temperature (Iglauer et al., 2014, Iglauer et al., 2015, Wan et al., 2014). The uncertainty of experimentally measured contact angle data in literature was analyzed and surface contamination was suggested as the main factor (Iglauer et al., 2014). A series of experiments with mica were conducted and several possible causes

of the ambiguity problem in contact angle measurement were suggested (Wan et al., 2014): surface chemistry changing due to cleaning or initial surface roughness, contamination by adsorbing contaminants, dissolution induced by phase disequilibrium, and water film altered by CO_2–brine–mineral reactions. Among these factors, phase disequilibrium may be overcome by fully saturating brine with CO_2 before experiments and carefully controlling during experiments. A recent study showed that phase equilibrium did not affect the contact angle within the first few minutes (Sarmadivaleh et al., 2015). The samples must be cleaned before experiments and as a result, samples may have different “history” based on different cleaning methods. Some “history” may change mineral wettability. Even a well-cleaned sample can be easily contaminated during transferring after cleaning. Surface contamination is difficult to control in experiments. A new protocol for contact angle measurement to distinguish advancing and receding contact angles was proposed (Sarmadivaleh et al., 2015). The measurement protocol may be one of the main causes of contact angle uncertainty. Molecular dynamics simulation (MDS) is a useful tool and has been used to investigate interfacial phenomena (Hamm et al., 2013, Iglauer et al., 2012, Liu et al., 2010, McCaughan et al., 2013, Tenney and Cygan, 2014, Tsuji et al., 2013, Yan et al., 2013). By using MDS, we can construct a mineral surface with a specific surface chemistry and get an absolutely clean surface that is difficult in experiments. In fact, MDS has already been used in predicting wettability of CO_2–brine–mineral systems. The pristine silica plane with silicon atoms in the outermost layer and its partly hydroxylated modification (surface hydroxyl density 1.6/nm^2) were used as a model hydrophobic surface and a model hydrophilic surface to predict wetting behavior at CO_2/water/silica interfaces (Liu et al., 2010). A fully hydroxylated silica surface was applied and contact angles between 29.9° and 52.4° when pressure ranged from 17 to 21 MPa were found (Bagherzadeh et al., 2012). Water contact angles on fully coordinated silica surface were predicted and contact angles about 80° under 10–15 MPa and 300 K for 1 M $CaCl_2$ solutions were found (Iglauer et al., 2012, McCaughan et al., 2013). Water/CO_2/hydrophilic silica systems at 296 K were simulated and contact angles about 20° at 13.9 MPa were got (Tsuji et al., 2013). Water contact angles on hydrophilic and hydrophobic basal surfaces of kaolinite were predicted (Tenney and Cygan, 2014). For kaolinite gibbsite surface, contact angles predicted by CO_2 droplet method were 169°, 180° and 180° for water, 0.78 M NaCl and 0.26 M $CaCl_2$, respectively. For kaolinite siloxane surface, contact angles predicted by CO_2 droplet method were 31°, 26° and 34° and values predicted by water droplet method were 145°, 141° and 145°, respectively. For CO_2/brine/silica systems, when supercritical CO_2 is in equilibrium with brine, the pH

value changes to about 3.0 (Kaszuba et al., 2003) and as a result, the formation of silanol sites is highly favorable (Hamm et al., 2013, Kim et al., 2012). Only three authors (Bagherzadeh et al., 2012, McCaughan et al., 2013, Tsuji et al., 2013) modeled silanol surfaces. However, they did not account for the effects of salinity.

In the present study, we investigated water contact angles on quartz surfaces using combined experimental and MDS methods. A divalent ion (Ca^{2+}) and a monovalent ion (Na^{+}) were used. The experimentally measured contact angles were compared with those predicted by MDS and the results were discussed.

2. Materials and methods

2.1. Experimental materials and apparatus

Fused quartz (Quartz Scientific Inc., purity of 99.995%, smooth, surface roughness <40 nm), ultra-pure DI water (resistivity ≥18 MΩ, Thermo Scientific Barnstead), CO_2 (Airgas, purity 99.99%), NaCl (ACS grade, Aldrich) and $CaCl_2{\cdot}2H_2O$ (ACS grade, Aldrich) were used in the experiments.

The experiments were conducted by using a high-pressure and high-temperature contact angle measurement apparatus (Fig. 1). A high P-T chamber (Temco, IFT-10) is the centerpiece. Inside the chamber, a stainless steel plate was welded horizontally at the center to hold a substrate by clipping onto the plate. The chamber was connected with a high P-T stirred Parr reactor (Model 4848) used to pre-saturate brine and CO_2. Two injection ports are located at the top and the bottom of the chamber allowing operating different fluid phases. Two syringe pumps (ISCO 500HP) were used, one was connected with the high-P-T chamber to control the pressure, and another was connected with the Parr reactor. Three inlets were connected with chamber for backup pressure regulation, water (brine) supply and CO_2 (captive drop method, pendant drop method) droplets making, respectively. A thermocouple was placed in the chamber and the chamber was covered by a heating belt (Diqi-Sense 8900-10). Viewing windows were opened on both sides. A high-speed camera (Nikon D7000) and a light source were placed outside of viewing windows to capture droplet shapes. To better control the temperature, the high P-T chamber together with the Parr reactor and the connected tubing for transferring the fluids were all sit inside a thermal insulation chamber.

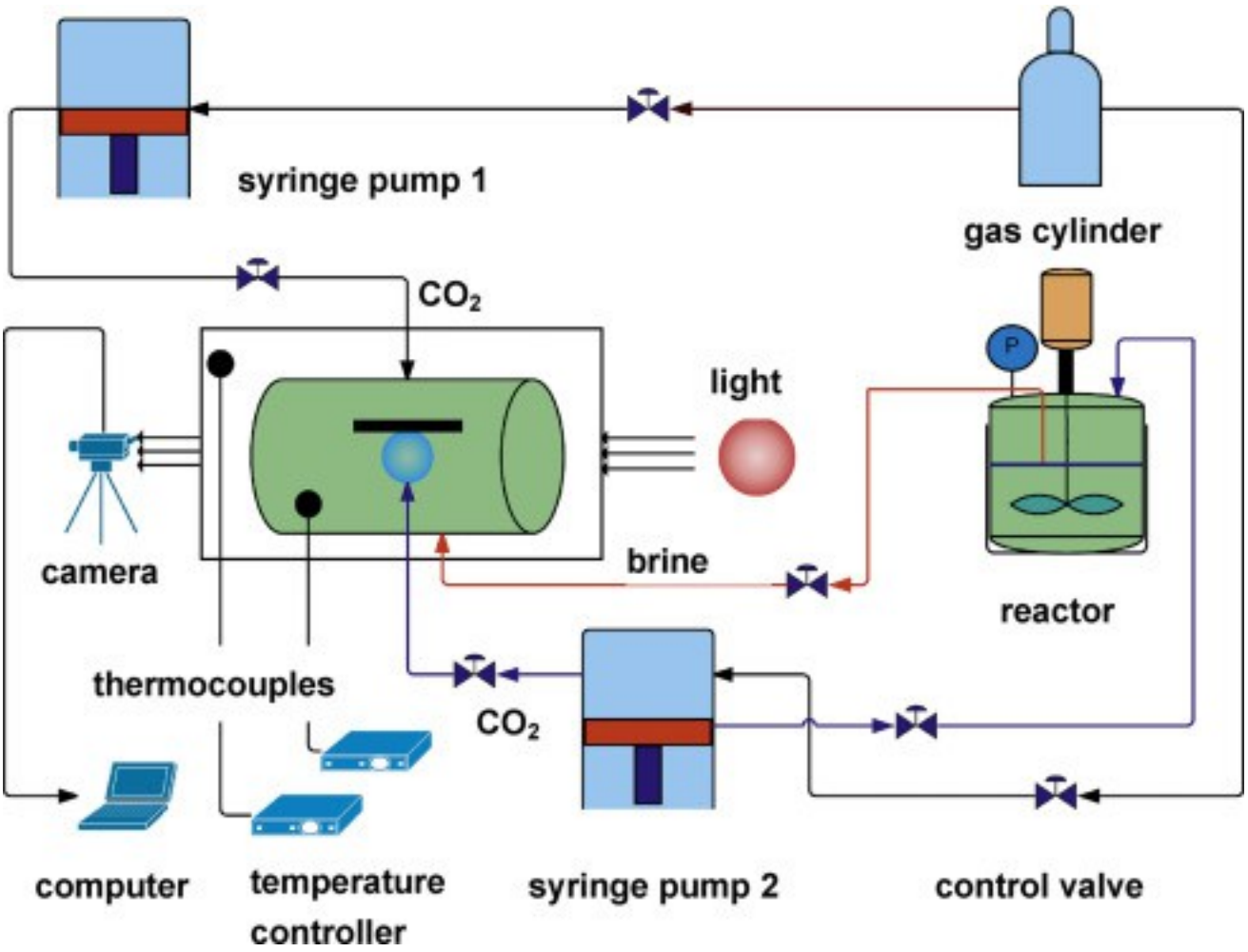

1. Download high-res image (309KB)
2. Download full-size image

Fig. 1. Chart of contact angle measurement apparatus for CO_2/brine/rock systems under high temperature and high pressure.

2.2. Experimental methods

The pendant drop method was used to measure static contact angles and the captive drop method was used to predict dynamic contact angles. Experiments were conducted under pressures between 7 and 18 MPa, temperatures 318–348 K and ionic strength 0–9 M using $CaCl_2$ (0–3 M) and NaCl (0–3 M). By using captive drop method to measure dynamic contact angles, the distance between needle and sample was carefully controlled in case CO_2 flux pass needle affected CO_2/brine/quartz interaction. Several tests were done to select proper distance before measurements.

Before contact angle measurements, it is important to prepare the mutually saturated brine and CO_2. We used the stirred Parr reactor for ≥12 h under the desired *P* and *T*.

Before an experiment, the high P-T chamber was thoroughly cleaned using acetone and DIW. The sample was cleaned with acetone and DIW before clipped onto the sample holder plate inside the chamber. It should be noted that, many cleaning methods have been used in contact angle measurement experiments: absolute ethanol and DIW (Kim et al., 2012), acetone and DIW (Wang et al., 2013a), strongly oxidizing chemicals and oxygen plasma (Al-Yaseri et al., 2015b), etc. The effect of cleaning protocols on contact angles is out of the scope of this study.

After loading the sample under the ambient conditions, the brine was injected to fill the chamber. Then, the chamber was pressurized and temperature was raised to the desired values. After the *P* and *T* reached to desired numbers, the liquid inside the chamber was 100% displaced by the CO_2–saturated brine from the Parr reactor under the same *P*–*T*. Then CO_2 from the Parr reactor was injected to displace 10% volume of the brine in order to have both fluids co-present inside the chamber. The chamber was maintained at the *P*–*T* for at least 2 h before the next step. CO_2 which had been fully saturated with water was slowly injected into the chamber through the bottom syringe to generate bubbles. For each experimental condition, two or three quartz plates were used and three to five CO_2 bubbles were measured for each plate. During static contact angle measurements, bubble shapes were captured for at least 2 h.

2.3. MDS methods

The silica surface which has been fully hydroxylated with a silanol number density of 9.4/$nm^2$was used as a model surface (Emami et al., 2014). The selection of model surface was discussed in the supplementary file (S0). The silica surfaces were first simulated in NPT ensemble at desired temperature and pressure before use. Equilibrium water and CO_2structures were used to construct a box with CO_2/water interfaces. The CO_2/water box was equilibrated in NPT ensemble at desired temperature and pressure to get a system with fully saturated water and CO_2. Different numbers of water molecules saturated with CO_2 or CO_2molecules saturated with water were selected to construct simulation cells.

The simulation cell contains three layers. A typical simulation cell for simulating water droplet on quartz surface under CO_2 atmosphere is illustrated in Fig. 2. The top and bottom layers are two identical quartz surfaces. The middle layer contains a water droplet in CO_2atmosphere or a CO_2 droplet in water. A half-cylindrical droplet geometry was used instead of the traditional spherical droplet method to better predict the contact angles (Rafiee et al., 2012). Both water droplet and CO_2 droplet were simulated in this study. The simulation cell used for simulating CO_2 droplet is similar to that for water

droplet. The only difference is that the middle layer is filled with a CO_2 droplet and water atmosphere.

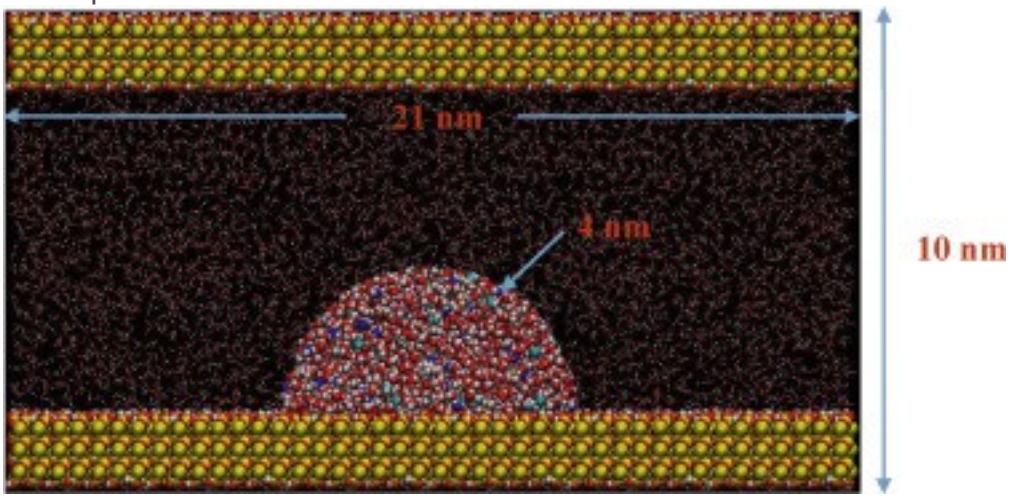

1. Download high-res image (751KB)
2. Download full-size image

Fig. 2. A snapshot of simulation cell used for simulating water droplet on quartz surface under CO_2atmosphere in *x-z* plane. Quartz, ions and water molecules were illustrated in VDW format, while CO_2molecules were drawn in CPK format.

For water droplet method, water molecules and CO_2 molecules that dissolved in water were selected from saturated water system with a half-cylindrical shape and then these molecules were placed on the bottom quartz layer. The rest of the middle layer space was filled with CO_2 molecules and water molecules that dissolved in selected from saturated CO_2 system. The procedure is similar for CO_2 droplet method. To remove interfacial stress generated by structure construction, molecules within the droplet were fixed and the cell was simulated in NVT ensemble at desired temperature. Then, similarly, molecules outside the droplet were fixed to remove stress between quartz surface and droplet. Finally, the simulation cell was run in NVT ensemble until configuration of the droplet no longer change with time. In all simulations, quartz molecules were fixed.

In the present study, eight simulation cells were constructed and parameters for these simulation cells were summarized in Table 1. Force field and other simulation details can be found in the supplementary file (S1 and S2). Two quartz surfaces were used and wall effects may affect the thermodynamic behavior of fluids and perhaps the contact angle values (Gelb and Gubbins, 2000). We discussed this issue in the supplementary file (S7).

2.4. Determination of contact angles

For experimental measurements, contact angles were calculated using an open source program ImageJ (http://rsb.info.nih.gov/ij). A contact angle plugin “DropSnake” (Stalder et al., 2006, Stalder et al., 2010) was applied. Several points were drawn automatically by snaking on the droplet boundary. And then these points were modified manually with the help of drop reflection. Finally, two contact angles (left and right contact points) were obtained by a piecewise polynomial fit. The determination methods of contact angles are similar to that used by other researchers (Wan et al., 2014, Wang et al., 2013a, Wang et al., 2013b).

For molecular dynamics simulations, contact angles were predicted using 2D density profiles of water. The density profiles were calculated based on a total 3 ns production run. CO_2–water contact curve was produced directly by density profiles. The quartz surface was defined as average positions for hydrogen atoms in silanol groups. Then the final 2D droplet and base surface were generated and contact angles were calculated based on tangent lines on both sides (Bagherzadeh et al., 2012). One density profile produces two contact angle data and three density profiles were generated in each simulation leading to a total of six data points for each simulation cell. The contact angles were averaged based on these data. Density profiles and tangent lines for contact angle prediction can be found in Section 3.2 and the supplementary file (S5).

3. Results and discussion

3.1. Contact angles measured by experiments

Water contact angles (both static and dynamic) were measured, and the results are summarized in Fig. 3, Fig. 4, Fig. 5. The measured static contact angle values are between advancing and receding angles as expected. For pressures from 7 to 18 MPa, temperatures from 318 to 348 K and salinity from 0 to 3 M, water contact angles are all below 30°, showing that quartz is strongly hydrophilic under these conditions. In the recent literatures the experimental measured contact angles from different laboratories varied up to around 90° (Iglauer et al., 2014). Recently, a higher water advancing contact angle of 47° was predicted under 13 MPa and 333 K (Al-Yaseri et al., 2015a). They used a sessile drop method and the advancing contact angles were predicted by adding water drops on the substrate to make a three phase line movement. The difference of water contact angles may be caused by different measurement methods and protocols.

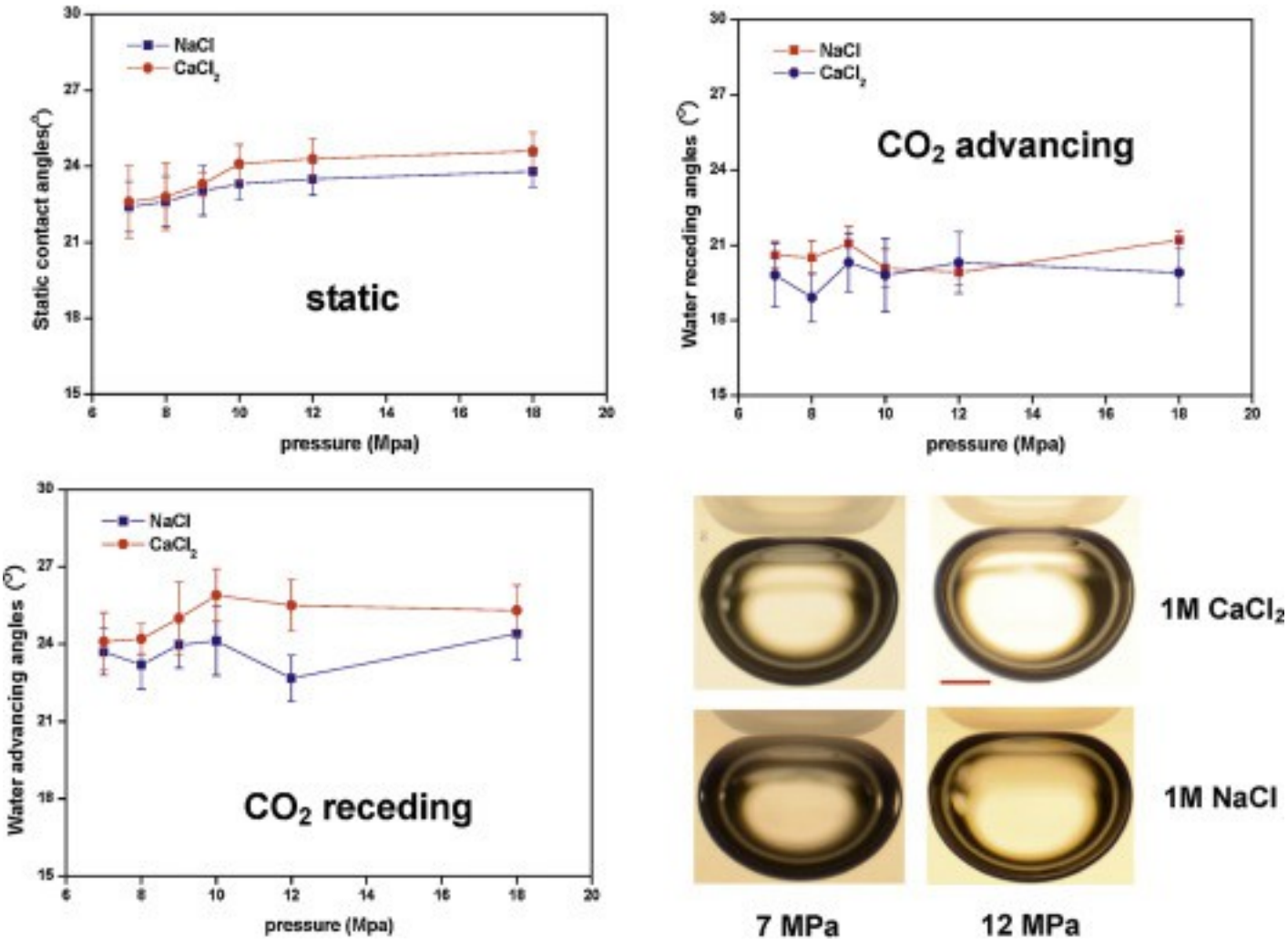

1. Download high-res image (402KB)
2. Download full-size image

Fig. 3. Water contact angles on quartz surface as a function of system pressure when ionic concentration is 1 M, temperature is 318 K for monovalent and divalent ions. Right bottom: photographs of CO_2 droplet on quartz surface during static contact angles measurement. A scale bar of 1 mm was shown.

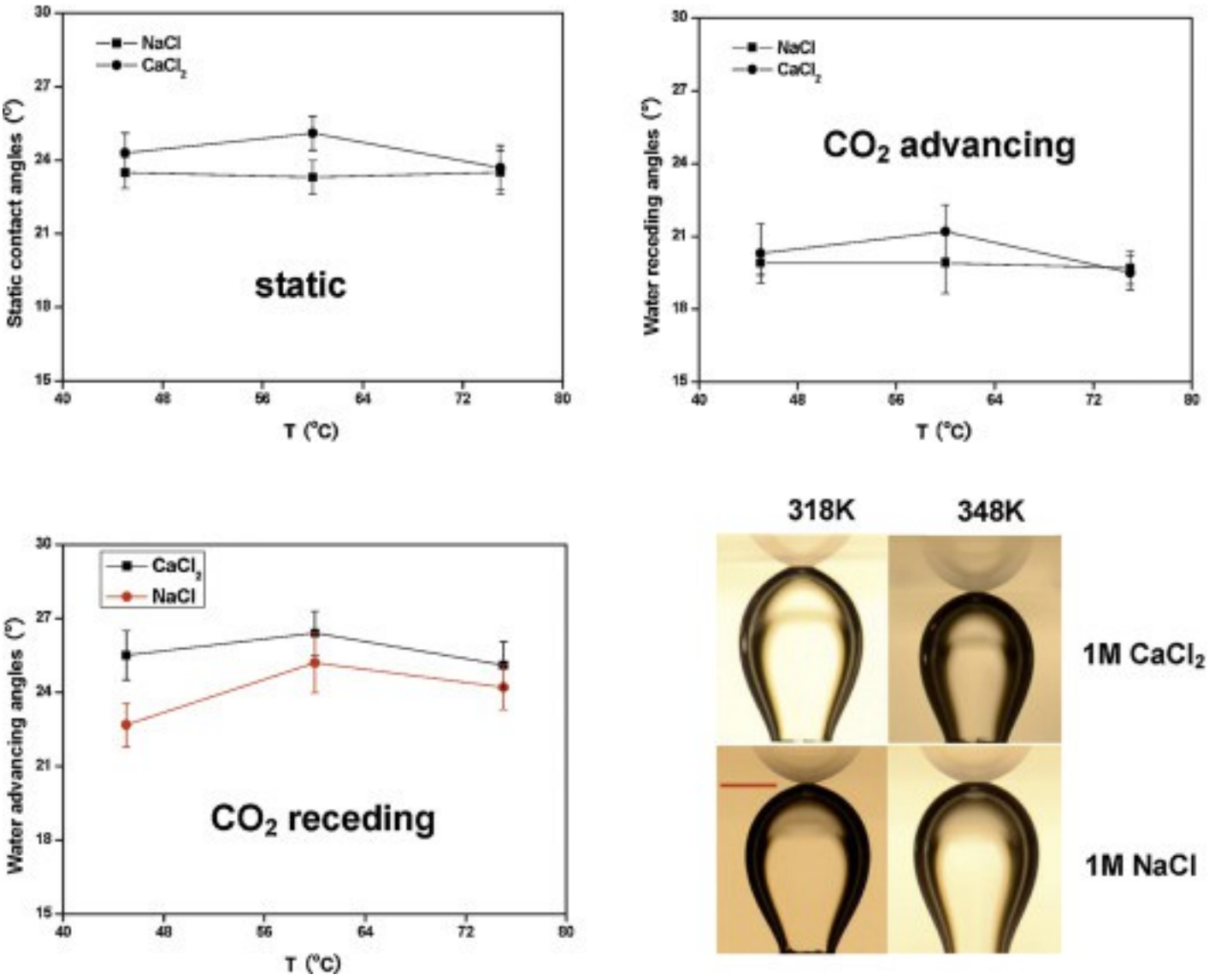

1. Download high-res image (368KB)
2. Download full-size image

Fig. 4. Water contact angles on quartz surface as a function of temperature when pressure is 12 MPa, ionic concentration is 1 M for monovalent and divalent ions. Right bottom: photographs of CO_2 droplet on quartz surface during dynamic contact angles measurement (water advancing). A scale bar of 1.5 mm was shown.

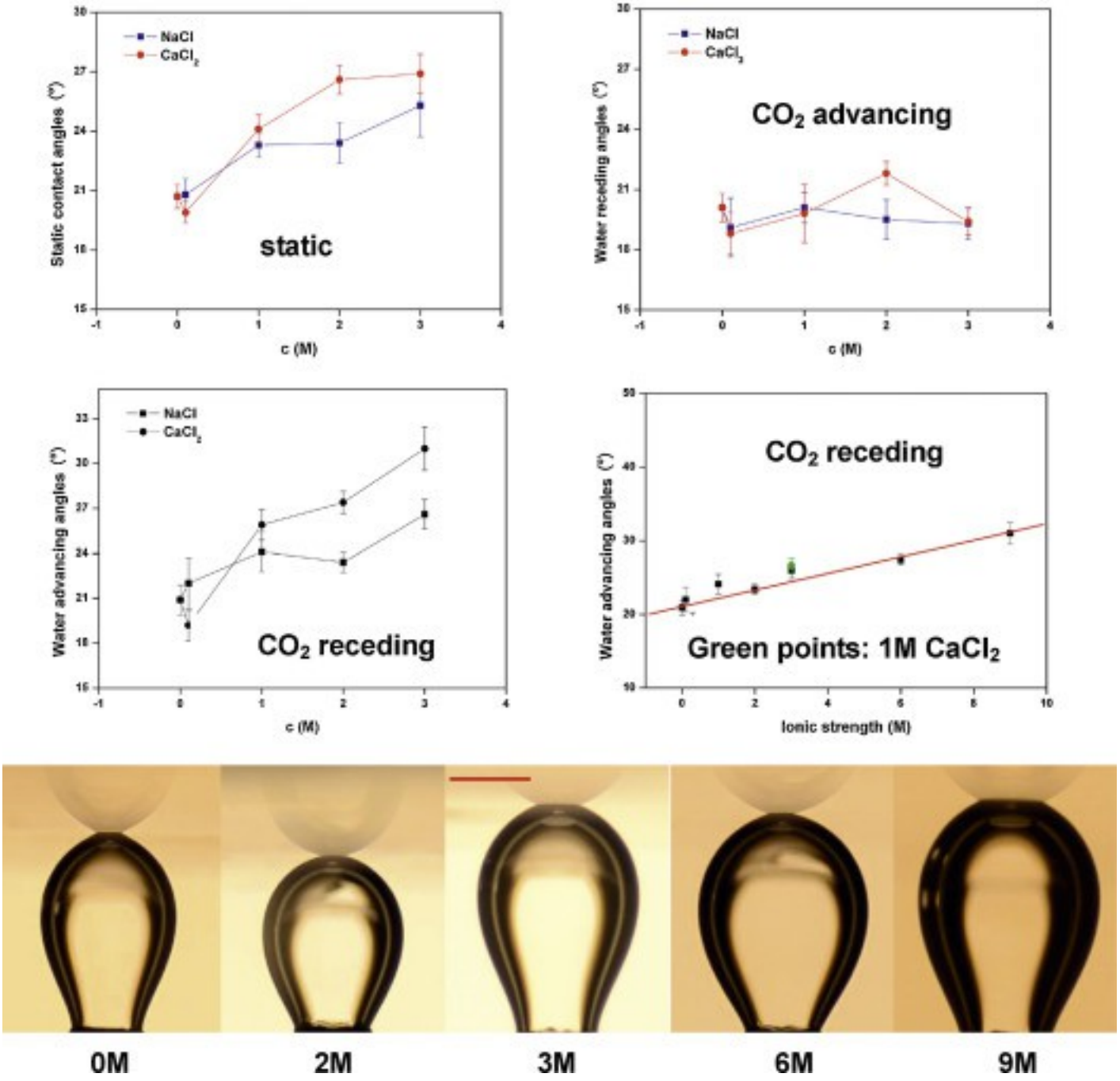

1. Download high-res image (523KB)
2. Download full-size image

Fig. 5. Water contact angles on quartz surface as a function of salinity and ionic strength when pressure is 10 MPa and temperature is 318 K. Photographs of CO_2 droplet during dynamic contact angles measurement (CO_2 receding) as a function of ionic strength are also given. A scale bar of 1.5 mm was shown.

Water contact angles as a function of pressure are shown in Fig. 3. The static and dynamic contact angles show no dependence on CO_2 pressure. The trends for NaCl and $CaCl_2$aqueous solutions are same. In fact, the pressure dependence of water contact angles is currently under debate: (1) Contact angles increase as pressure increases in the region of phase transition (7–10 MPa), and there is no or little pressure dependence in liquid and supercritical region (Dickson et al., 2006, Jung and Wan, 2012, Saraji et al., 2013, Sutjiadi-Sia et al., 2008). (2) A continuous increasing of water contact angles with pressure increasing: 0–11 MPa (Chiquet et al., 2007), 0–31 MPa (Yang et al., 2008), 0–20 MPa (Al-Yaseri et al., 2015b) and 0–15 MPa (Iglauer et al., 2014). (3) Water contact angles are pressure independence: 0–10 MPa (Chalbaud et al., 2009, Espinoza and Santamarina, 2010), 0–30 MPa (Farokhpoor et al., 2013), 0–14 MPa (Kaveh et al., 2014) and 13.8–27.6 MPa (Saraji et al., 2014). (4) Water contact angles decrease as CO_2 pressure increases in liquid phase: calcite (Espinoza and Santamarina, 2010) and quartz (Bikkina, 2011). Our measured static contact angles (experimental pressure 7–20 MPa) show slight increase in the pressure region 7–10 MPa and independent of the pressure when pressure continues to increase.

Water contact angles as a function of temperature for 1 M solutions are illustrated in Fig. 4. The measured static contact angles are around 24° showing a temperature independent trend considering the experimental errors. Water receding and advancing angles follow the same trend. It seems that ion type has no effect on the temperature dependence of water contact angles. These experimental results agree well with those published in literature (Farokhpoor et al., 2013, Saraji et al., 2014). Recent studies showed that advancing water contact angles increased significantly with temperature increase (Al-Yaseri et al., 2015b, Sarmadivaleh et al., 2015). However, they applied a sessile drop method and water advancing contact angles were generated by adding several water drops (Sarmadivaleh et al., 2015) and tilting-plate technique (Al-Yaseri et al., 2015b), respectively.

The water contact angles as a function of salinity were summarized in Fig. 5. Similar to results in literature (Espinoza and Santamarina, 2010, Farokhpoor et al., 2013, Jung and Wan, 2012, Kim et al., 2012, Saraji et al., 2014, Wang et al., 2013a), increasing brine salinity induces an increase in water contact angles. For NaCl aqueous solutions, water contact angle increases from 21° to 25° when salinity increases from 0 to 3 M. However, for $CaCl_2$aqueous solutions, water contact angle increases 6° within the same salinity range. For dynamic contact angles, water receding angles change slightly with salinity, but water advancing angles show a strong dependence with salinity. A recent study found a different trend where receding angles also changed significantly with

salinity, but they used a tilting-plate technique to measure dynamic contact angles which is different from the technique used in the present study (Al-Yaseri et al., 2015b). For NaCl and $CaCl_2$ aqueous solutions, when salinity increases from 0 to 3 M, water advancing angles increase 6° and 10°, respectively. The difference is due to different ionic strength for the same ions concentration showing a strong dependence of contact angle on ionic strength. A linear relationship can be found between water advancing angles and ionic strength and a linear fit leads to $\theta = 21.04 + 1.13I$ (I:°/M, $R = 0.94$). For static contact angles, the slope decreases to 0.84 ($R = 0.91$). A similar linear relationship with a slope of 4 has been found (Jung and Wan, 2012). It should be noted that water contact angles they measured were much larger than that reported here.

3.2. Contact angles predicted by molecular dynamics simulations

3.2.1. Salinity dependence

Molecular dynamics simulations were performed with simulation cells 1–8. Four salinity were considered under 0 M and 3 M $CaCl_2$, 3 M NaCl, and 1 M $CaCl_2$. The temperature was fixed at 318 K. As the NVT ensemble was used in contact angles prediction simulation, the pressures were estimated according to final CO_2 density. CO_2 densities were calculated and averaged in bulk CO_2 (water droplet method: 10 Å or more away from quartz surface and water droplet; CO_2 droplet method: central CO_2 droplet). The pressures were estimated based on NIST data book for CO_2 (www.nist.gov). For cells 1–4, the calculated CO_2densities were 587.6 (5.5), 593.8 (7.6), 597.1 (6.3) and 583.9 (5.4) kg/m^3, respectively and these data correspond to 10.8, 10.9, 10.9 and 10.8 MPa. Fully hydroxylated silica surface is hydrophilic (Duval et al., 2002, Emami et al., 2014). As expected, water droplets wet the silica surface on all conditions studied. Water droplet spreading with simulation time can be found in the supplementary file (S3). When water droplet shape stopped to change with time, density profiles were produced. Then water contact angles were calculated based on density profiles. The results for pure water droplets are illustrated in Fig. 6, indicating the predicted water contact angle is 22.6° which agrees well with experimental results in this study (20–21°). Our result is also in accord with other molecular dynamics simulation predictions (Tsuji et al., 2013): 20° under 296 K and 13.9 MPa. A similar hydroxylated silica surface was also used by other authors, but they got water contact angles nearly 30° for water (Bagherzadeh et al., 2012). It should be noted that they used different initial setup and much shorter simulation time (2 ns). Several authors applied different silica surfaces and their predicted results were between 60° and 90° (Iglauer et al., 2012, Liu et al., 2010, McCaughan et al., 2013).

The results for water droplets of 3 M $CaCl_2$ and 3 M NaCl are presented in Fig. 7, Fig. 8, respectively. When salinity increases to 3 M, water contact angles increase to 29.5° and 35.5° for NaCl and $CaCl_2$ aqueous solutions, respectively. These values are reasonable compared with experimental results (20–27° and 20–31°). The water contact angle for 1 M $CaCl_2$ solution has also been predicted and the results are illustrated in the supplementary file (S5). The predicted value is 28.7° and agrees well with the experimental result of 20–26°. Much higher water contact angles (about 80°) were predicted at 300 K and pressures from 10 to 20 MPa (McCaughan et al., 2013). But they used a half-hydroxylated quartz surface (silanol density around 4.6 OH/nm^2) and a fully coordinated quartz surface. It should be noted that to the best of our knowledge, there are no MDS predictions of water contact angles on fully hydroxylated quartz for NaCl and $CaCl_2$ aqueous solutions, and we cannot compare our results with other MDS studies. However, the accordance of our simulation results with experimental results shows that molecular dynamics simulation is a good tool to predict contact angles as long as proper simulation protocol and force field are selected and the results are quantitatively comparable with experimental results.

Due to the hydrophilic nature of fully hydroxylated silica surface, CO_2 droplets with initial cylindrical geometry dewet from the surface. A clear dewetting with simulation time was found during MDS, however, CO_2 droplets finally detached from the surface. As a result, it is impossible to predict contact angles using CO_2 droplet method. The dewetting process of CO_2 droplet and density profiles can be found in the supplementary file (S4 and S6). The final CO_2 droplet shapes were summarized in Fig. 9. The detaching distances are different with the order of pure water > 3 M NaCl (1 M $CaCl_2$) > 3 M $CaCl_2$. In fact, this is caused by different water contact angles. A similar phenomenon was found during simulating contact angles on basal surfaces of kaolinite using a CO_2 droplet method (Tenney and Cygan, 2014).

3.2.2. Pressure and temperature dependence

To study the effects of pressure and temperature, three additional simulation runs were produced. The final coordination files for simulation cell 2 (after 15 ns run) were used as a start point. The number of CO_2 molecules was modified to change bulk CO_2 density according to desired pressure. Two pressures were considered: 7 MPa and 9.6 MPa with the constant temperature 318 K, and 10.9 MPa at 333 K.

The predicted water contact angles for different pressures are 32.2° (±2.8) and 35.8° (±4.3), respectively. The calculated water contact angle at 333 K was 36.2° (±4.1). As shown in Fig. 7, water contact angles for simulation cell 2 at 10.9 MPa and 318 K is

35.5°(±3.6). These data implies that water contact angles show no dependence with pressure and temperature as found by our experimental results.

3.2.3. MDS prediction of contact angles on "CO_2-reacted" quartz surface

CO_2 sorption on silica surfaces were studied by experiments (Di Giovanni et al., 2001, McCool and Tripp, 2005, Roque-Malherbe et al., 2010, Tripp and Combes, 1998) and molecular simulation studies (Vishnyakov et al., 2008). To study the effect of CO_2 pre-reaction on wettability, we conduct simulations with CO_2-reacted quartz surface. It should be noted that, the reaction mentioned here is physic-sorption and functional groups on quartz surface are not changed.

At first, water cylindrical droplet in simulation cell 2 (initial structure, not equilibrated) was removed and replaced by CO_2 molecules to form a new simulation cell containing CO_2 and quartz. The new generated cell was simulated in NVT ensemble for 12 ns to obtain an equilibrium structure containing CO_2 and pre-reacted quartz surface. Then, water cylindrical droplet was placed into the equilibrium structure by removing a certain number of CO_2molecules. In order not to change the CO_2-quartz structure near the quartz surface, water droplet was placed above surface with a distance of 8 Å. The new cell with water droplet was simulated and water contact angles were calculated.

The snapshots of water droplets as a function of simulation time were illustrated in Fig. 10. The CO_2-layer was displaced by water molecules quickly (less than 2 ns). However, a small amount of CO_2 molecules were left between quartz surface and water molecules at the middle bottom of the droplet. The number of captured CO_2 molecules decreased as simulation went on. But the speed was rather slow. In the meantime, water molecules spread on quartz surface and the droplet shape became same as that in Fig. 7 after 10 ns. This implies that the CO_2 layer after CO_2-quartz pre-reaction does not change wettability. It has been proposed that physic-sorption (Dickson et al., 2006) and/or hydrogen bonds (Vishnyakov et al., 2008) between CO_2 and quartz exist. Based on our results, the physic-sorption and hydrogen bonds between CO_2 and quartz seems very weak compared with water-quartz interaction. It should be noted that we used a flat fully hydroxylated surface and the roughness was not considered.

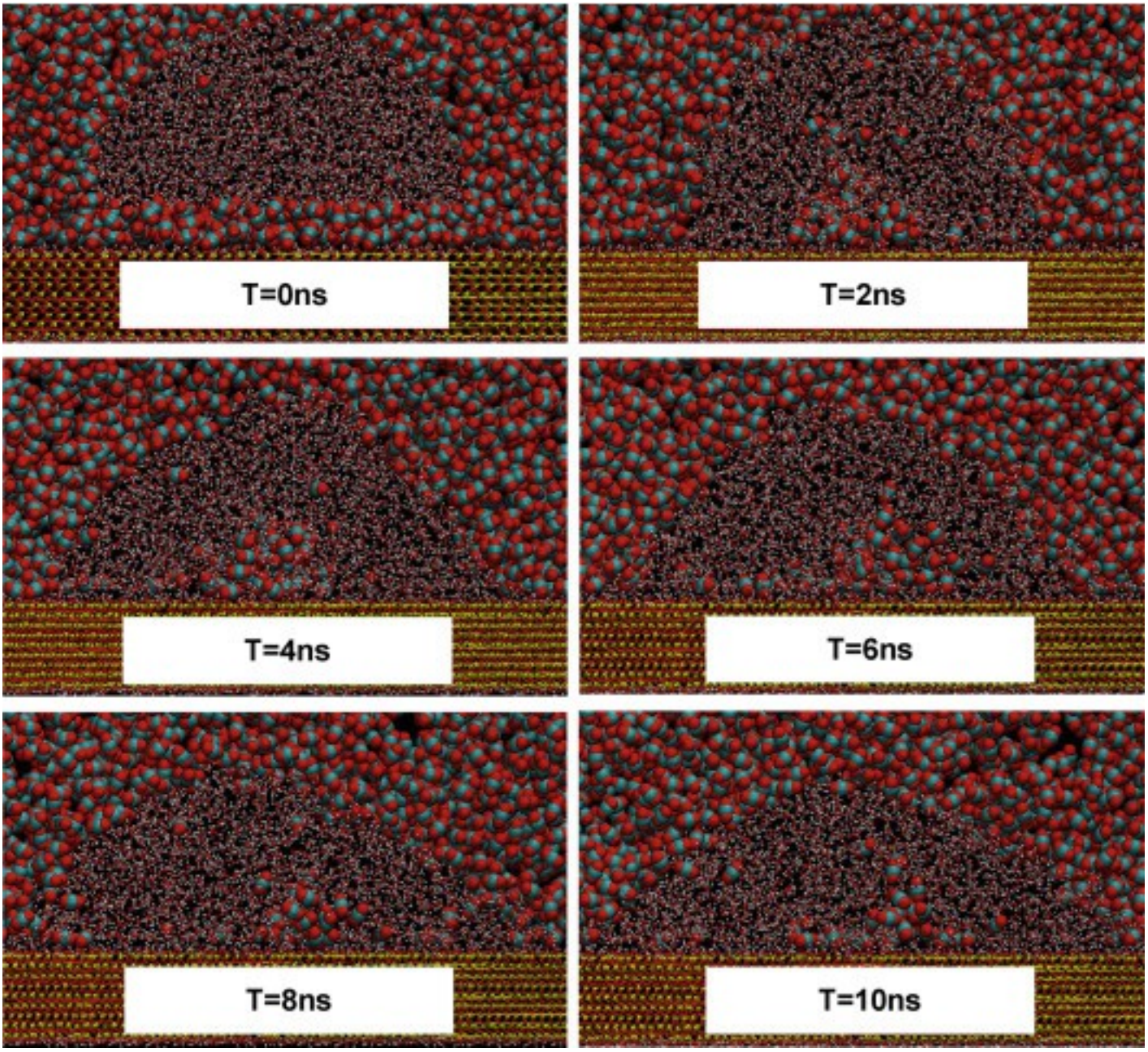

1. Download high-res image (3MB)
2. Download full-size image

Fig. 10. Snapshots of water droplets as a function of simulation time. The water droplet was initially placed above the quartz surface at a distance of 8 Å. The snapshots are in *x-z* plane. For clarity, salt ions are not shown.

4. Conclusions

Static and dynamic contact angles of supercritical CO_2 and brine on quartz surface under CO_2 sequestration conditions were investigated using a high-pressure and high-

temperature contact angle measurement apparatus. The results show that water contact angles increases as ionic strength increases. However, the effects of pressure and temperature are insignificant. The trend of the dependence of ionic strength, pressure and temperature seems to be the same for monovalent and divalent ions solutions.
Water static contact angles were studied using molecular dynamics simulation methods. The predicted water contact angles agree well with those obtained by laboratory measurements. The results of molecular dynamics simulation are qualitatively consistent with the experimental results, indicating that molecular dynamics simulation is a suitable tool for predicting water contact angles under CO_2 sequestration conditions. Due to the ambiguity during contact angle experimental measurements, molecular dynamics simulation can become very useful to help improve our understanding of wettability on mineral surface for CO_2/brine systems.
Water contact angles on a flat, CO_2 pre-reacted quartz surface have also been simulated. The results show that the adsorbed CO_2 on quartz surface can be easily replaced by water droplet. The final water contact angle does not change although some CO_2 molecules are captured. The results on rough surface maybe different and further studies are required.
A fully hydroxylated quartz surface was applied during molecular dynamics simulations. The accordance of experimental and simulation results shows that under these experimental conditions, silanol groups are dominant on quartz surface. Under real CO_2 sequestration environment, the functional groups on quartz surface are complex: Si–O–H, Si–O–Si, Si–O-ions and their combination (Emami et al., 2014). It has been shown that siloxane is hydrophobic (Tenney and Cygan, 2014) and wettability depends on the ratio of silanol vs. siloxane (Emami et al., 2014). Further investigation should be made on quartz surface with different functional groups to better understand wettability alteration caused by contamination and/or CO_2 reactions.

Acknowledgements

This research was supported by the following projects: project 51206016 funded by National Natural Science Foundation of China (NSFC), the Doctoral Startup Funds of Liaoning Province (20121021) and the Fundamental Research Funds for the Central Universities(DUT14LAB13). Grateful acknowledge should be sent to China Scholarship Council for the financial support for Dr. Chen during staying in U.S.A. Dr. Wan's involvement in this work and the laboratory facility were supported by the Center for Nanoscale Control of Geologic CO_2, an Energy Frontier Research Center funded by the U.S. Department of Energy, Office of Science, and Office of Basic Energy

Sciences under Award Number DE-AC02-05CH11231. Thank Tetsu K. Tokunaga (Lawrence Berkeley National Lab) for reading this manuscript and helpful comments. We thank Drs. Yongman Kim, Shibo Wang, Prem Bikkina and Wenming Dong (Lawrence Berkeley National Lab) for the kind help during experiments, and the fruitful discussion on contact angle experiments. We also thank Computing Center in Department of Energy and Power Engineering of Dalian University of Technology for providing parallel computing environment.

Appendix A. Supplementary data

The following are the supplementary data to this article:

Download Word document (4MB)Help with doc files

References

Al-Yaseri et al., 2015a

A. Al-Yaseri, M. Sarmadivaleh, A. Saeedi, M. Lebedev, A. Barifcani, S. Iglauer**N-2 + CO_2 + NaCl brine interfacial tensions and contact angles on quartz at CO_2 storage site conditions in the Gippsland basin, Victoria/Australia**

J. Pet. Sci. Eng., 129 (2015), pp. 58-62

ArticleDownload PDFView Record in Scopus

Al-Yaseri et al., 2015b

A.Z. Al-Yaseri, M. Lebedev, A. Barifcani, S. Iglauer**Receding and advancing (CO_2 + brine + quartz) contact angles as a function of pressure, temperature, surface roughness, salt type and salinity**

J. Chem. Thermodyn. (2015), 10.1016/j.jct.2015.07.031

Altman et al., 2014

S.J. Altman, B. Aminzadeh, M.T. Balhoff, P.C. Bennett, S.L. Bryant, M.B. Cardenas, K.Chaudhary, R.T. Cygan, W. Deng, T. Dewers, D.A. DiCarlo, P. Eichhubl, M.A. Hesse, C. Huh, E.N.Matteo, Y. Mehmani, C.M. Tenney, H. Yoon**Chemical and hydrodynamic mechanisms for long-term geological carbon storage**

J. Phys. Chem. C, 118 (2014), pp. 15103-15113

CrossRefView Record in Scopus

Andrew et al., 2014

M. Andrew, B. Bijeljic, M.J. Blunt**Pore-scale contact angle measurements at reservoir conditions using X-ray microtomography**

Adv. Water Resour., 68 (2014), pp. 24-31

ArticleDownload PDFView Record in Scopus

Bagherzadeh et al., 2012

S.A. Bagherzadeh, P. Englezos, S. Alavi, J.A. Ripmeester**Influence of hydrated silica surfaces on interfacial water in the presence of clathrate hydrate forming gases**
J. Phys. Chem. C, 116 (2012), pp. 24907-24915
CrossRefView Record in Scopus

Bikkina, 2011

P.K. Bikkina**Contact angle measurements of CO_2-water-quartz/calcite systems in the perspective of carbon sequestration**
Int. J. Greenh. Gas Control, 5 (2011), pp. 1259-1271
ArticleDownload PDFView Record in Scopus

Bikkina, 2012

P.K. Bikkina**Reply to the comments on "Contact angle measurements of CO_2-water-quartz/calcite systems in the perspective of carbon sequestration"**
Int. J. Greenh. Gas Control, 7 (2012), pp. 263-264
ArticleDownload PDFView Record in Scopus

Chalbaud et al., 2009

C. Chalbaud, M. Robin, J.-M. Lombard, F. Martin, P. Egermann, H. Bertin**Interfacial tension measurements and wettability evaluation for geological CO_2 storage**
Adv. Water Resour., 32 (2009), pp. 98-109
ArticleDownload PDFView Record in Scopus

Chiquet et al., 2007

P. Chiquet, D. Broseta, S. Thibeau**Wettability alteration of caprock minerals by carbon dioxide**
Geofluids, 7 (2007), pp. 112-122
CrossRefView Record in Scopus

Di Giovanni et al., 2001

O. Di Giovanni, W. Dorfler, M. Mazzotti, M. Morbidelli**Adsorption of supercritical carbon dioxide on silica**
Langmuir, 17 (2001), pp. 4316-4321
CrossRefView Record in Scopus

Dickson et al., 2006

J.L. Dickson, G. Gupta, T.S. Horozov, B.P. Binks, K.P. Johnston**Wetting phenomena at the CO_2/water/glass interface**
Langmuir, 22 (2006), pp. 2161-2170
CrossRefView Record in Scopus

Duval et al., 2002

Y. Duval, J.A. Mielczarski, O.S. Pokrovsky, E. Mielczarski, J.J. Ehrhardt**Evidence of the existence of three types of species at the quartz-aqueous solution interface at pH 0–10: XPS surface group quantification and surface complexation modeling**

J. Phys. Chem. B, 106 (2002), pp. 2937-2945
CrossRefView Record in Scopus

Emami et al., 2014

F.S. Emami, V. Puddu, R.J. Berry, V. Varshney, S.V. Patwardhan, C.C. Perry, H. Heinz**Force field and a surface model database for silica to simulate interfacial properties in atomic resolution**
Chem. Mater., 26 (2014), pp. 2647-2658
CrossRefView Record in Scopus

1
0

D.N. Espinoza, J.C. Santamarina**Water-CO_2-mineral systems: interfacial tension, contact angle, and diffusion – implications to CO_2geological storage**
Water Resour. Res., 46 (2010), p. W07537
View Record in Scopus

Farokhpoor et al., 2013

R. Farokhpoor, B.J.A. Bjorkvik, E. Lindeberg, O. Torsaeter**Wettability behaviour of CO_2 at storage conditions**
Int. J. Greenh. Gas Control, 12 (2013), pp. 18-25
ArticleDownload PDFView Record in Scopus

Gelb and Gubbins, 2000

L.D. Gelb, K.E. Gubbins**Phase separation in confined systems (vol 62, pg 1573, 1999)**
Rep. Prog. Phys., 63 (2000), p. 727
CrossRef

Hamm et al., 201

L.M. Hamm, I.C. Bourg, A.F. Wallace, B. Rotenberg**Molecular simulation of CO_2- and CO_3-brine-mineral systems**
D.J. DePaolo, D.R. Cole, A. Navrotsky, I.C. Bourg (Eds.), Geochemistry of Geologic CO_2 Sequestration, Mineralogical Soc. Amer., Chantilly (2013), pp. 189-228
CrossRefView Record in Scopus

Iglauer et al., 201

S. Iglauer, M.S. Mathew, F. Bresme**Molecular dynamics computations of brine–CO_2 interfacial tensions and brine–CO_2–quartz contact angles and their effects on structural and residual trapping mechanisms in carbon geo-sequestration**
J. Colloid Interface Sci., 386 (2012), pp. 405-414
ArticleDownload PDFView Record in Scopus

Iglauer et al., 201

S. Iglauer, C.H. Pentland, A. Busch**CO_2 wettability of seal and reservoir rocks and the implications for carbon geo-sequestration**
Water Resour. Res., 51 (2015), pp. 729-774
CrossRefView Record in Scopus

Iglauer et al., 201

S. Iglauer, A. Salamah, M. Sarmadivaleh, K.Y. Liu, C. Phan**Contamination of silica surfaces: impact on water–CO_2–quartz and glass contact angle measurements**

Int. J. Greenh. Gas Control, 22 (2014), pp. 325-328
ArticleDownload PDFView Record in Scopus

Jung and Wan, 2

J.-W. Jung, J. Wan**Supercritical CO_2 and ionic strength effects on wettability of silica surfaces: equilibrium contact angle measurements**
Energy Fuels, 26 (2012), pp. 6053-6059
CrossRefView Record in Scopus

Kaszuba et al., 2

J.P. Kaszuba, D.R. Janecky, M.G. Snow**Carbon dioxide reaction processes in a model brine aquifer at 200 degrees C and 200 bars: implications for geologic sequestration of carbon**
Appl. Geochem., 18 (2003), pp. 1065-1080
ArticleDownload PDFView Record in Scopus

Kaveh et al., 201

N.S. Kaveh, E.S.J. Rudolph, P. van Hemert, W.R. Rossen, K.H. Wolf**Wettability evaluation of a CO_2/water/Bentheimer sandstone system: contact angle, dissolution, and bubble size**
Energy Fuels, 28 (2014), pp. 4002-4020
CrossRef

Kim and Santam

S. Kim, J.C. Santamarina**Engineered CO_2 injection: the use of surfactants for enhanced sweep efficiency**
Int. J. Greenh. Gas Control, 20 (2014), pp. 324-332
ArticleDownload PDFView Record in Scopus

Kim et al., 2012

Y. Kim, J.M. Wan, T.J. Kneafsey, T.K. Tokunaga**Dewetting of silica surfaces upon reactions with supercritical CO_2 and brine: pore-scale studies in micromodels**
Environ. Sci. Technol., 46 (2012), pp. 4228-4235
CrossRefView Record in Scopus

Liu et al., 2010

S. Liu, X. Yang, Y. Qin**Molecular dynamics simulation of wetting behavior at CO_2/water/solid interfaces**
Chin. Sci. Bull., 55 (2010), pp. 2252-2257
CrossRefView Record in Scopus

Mahadevan, 201

J. Mahadevan**Comments on the paper titled “Contact angle measurements of CO_2-water-quartz/calcite systems in the perspective of carbon sequestration”: a case of contamination?**
Int. J. Greenh. Gas Control, 7 (2012), pp. 261-262
ArticleDownload PDFView Record in Scopus

McCaughan et a

J. McCaughan, S. Iglauer, F. Bresme**Molecular dynamics simulation of water/CO_2-quartz interfacial properties: application to subsurface gas injection**
Energy Proc., 37 (2013), pp. 5387-5402
ArticleDownload PDFView Record in Scopus

McCool and Trip

B. McCool, C.P. Tripp**Inaccessible hydroxyl groups on silica are accessible in supercritical CO_2**
J. Phys. Chem. B, 109 (2005), pp. 8914-8919
CrossRefView Record in Scopus

Michael et al., 20

K. Michael, A. Golab, V. Shulakova, J. Ennis-King, G. Allinson, S. Sharma, T. Aiken**Geological storage of CO_2 in saline aquifers – a review of the experience from existing storage operations**
Int. J. Greenh. Gas Control, 4 (2010), pp. 659-667
ArticleDownload PDFView Record in Scopus

Rafiee et al., 201

J. Rafiee, X. Mi, H. Gullapalli, A.V. Thomas, F. Yavari, Y.F. Shi, P.M. Ajayan, N.A. Koratkar**Wettin g transparency of graphene**
Nat. Mater., 11 (2012), pp. 217-222
CrossRefView Record in Scopus

Roque-Malherbe

R. Roque-Malherbe, R. Polanco-Estrella, F. Marquez-Linares**Study of the interaction between silica surfaces and the carbon dioxide molecule**
J. Phys. Chem. C, 114 (2010), pp. 17773-17787
CrossRefView Record in Scopus

Saraji et al., 201

S. Saraji, L. Goual, M. Piri, H. Plancher**Wettability of supercritical carbon dioxide/water/quartz systems: simultaneous measurement of contact angle and interfacial tension at reservoir conditions**
Langmuir, 29 (2013), pp. 6856-6866
CrossRefView Record in Scopus

Saraji et al., 201

S. Saraji, M. Piri, L. Goual**The effects of SO_2 contamination, brine salinity, pressure, and temperature on dynamic contact angles and interfacial tension of supercritical CO_2/brine/quartz systems**
Int. J. Greenh. Gas Control, 28 (2014), pp. 147-155
ArticleDownload PDFView Record in Scopus

Sarmadivaleh et

M. Sarmadivaleh, A.Z. Al-Yaseri, S. Iglauer**Influence of temperature and pressure on quartz–water–CO_2 contact angle and CO_2–water interfacial tension**
J. Colloid Interface Sci., 441 (2015), pp. 59-64
ArticleDownload PDFView Record in Scopus

Song and Zhang

J. Song, D.X. Zhang**Comprehensive review of caprock-sealing mechanisms for geologic carbon sequestration**
Environ. Sci. Technol., 47 (2013), pp. 9-22
CrossRefView Record in Scopus

Stalder et al., 20

A.F. Stalder, G. Kulik, D. Sage, L. Barbieri, P. Hoffmann**A snake-based approach to accurate determination of both contact points and contact angles**
Colloid Surf. A: Physicochem. Eng. Asp., 286 (2006), pp. 92-103
ArticleDownload PDFView Record in Scopus

Stalder et al., 20

A.F. Stalder, T. Melchior, M. Mueller, D. Sage, T. Blu, M. Unser**Low-bond axisymmetric drop shape analysis for surface tension and contact angle measurements of sessile drops**
Colloid Surf. A: Physicochem. Eng. Asp., 364 (2010), pp. 72-81
ArticleDownload PDFView Record in Scopus

Sutjiadi-Sia et al

Y. Sutjiadi-Sia, P. Jaeger, R. Eggers**Interfacial phenomena of aqueous systems in dense carbon dioxide**
J. Supercrit. Fluids, 46 (2008), pp. 272-279
ArticleDownload PDFView Record in Scopus

Tenney and Cyg

C.M. Tenney, R.T. Cygan**Molecular simulation of carbon dioxide, brine, and clay mineral interactions and determination of contact angles**
Environ. Sci. Technol., 48 (2014), pp. 2035-2042
CrossRefView Record in Scopus

Tokunaga and W

T.K. Tokunaga, J.M. Wan**Capillary pressure and mineral wettability influences on reservoir CO_2 capacity**
D.J. DePaolo, D.R. Cole, A. Navrotsky, I.C. Bourg (Eds.), Geochemistry of Geologic CO_2 Sequestration, Mineralogical Soc. Amer., Chantilly (2013), pp. 481-503
CrossRefView Record in Scopus

Tripp and Combe

C.P. Tripp, J.R. Combes**Chemical modification of metal oxide surfaces in supercritical CO_2: the interaction of supercritical CO_2 with the adsorbed water layer and the surface hydroxyl groups of a silica surface**

Langmuir, 14 (1998), pp. 7350-7352
View Record in Scopus

Tsuji et al., 2013
S. Tsuji, Y.F. Liang, M. Kunieda, S. Takahashi, T. Matsuoka**Molecular dynamics simulations of the CO_2–water–silica interfacial systems**
Energy Proc., 37 (2013), pp. 5435-5442
(GHGT-11)
ArticleDownload PDFView Record in Scopus

Vishnyakov et al
A. Vishnyakov, Y.Y. Shen, M.S. Tomassone**Interactions of silica nanoparticles in supercritical carbon dioxide**
J. Chem. Phys., 129 (2008)

Wan et al., 2014
J.M. Wan, Y. Kim, T.K. Tokunaga**Contact angle measurement ambiguity in supercritical CO_2-water-mineral systems: mica as an example**
Int. J. Greenh. Gas Control, 31 (2014), pp. 128-137
ArticleDownload PDFView Record in Scopus

Wang et al., 201
S.B. Wang, I.M. Edwards, A.F. Clarens**Wettability phenomena at the CO_2–brine–mineral interface: implications for geologic carbon sequestration**
Environ. Sci. Technol., 47 (2013), pp. 234-241
CrossRefView Record in Scopus

Wang et al., 2013b
S.B. Wang, Z.Y. Tao, S.M. Persily, A.F. Clarens**CO_2 adhesion on hydrated mineral surfaces**
Environ. Sci. Technol., 47 (2013), pp. 11858-11865
CrossRefView Record in Scopus

Yan et al., 2013
M.Q. Yan, X.N. Yang, Y.J. Lu**Wetting behavior of water droplet on solid surfaces in solvent environment: a molecular simulation study**
Colloid Surf. A: Physicochem. Eng. Asp., 429 (2013), pp. 142-148
ArticleDownload PDFView Record in Scopus

Yang et al., 2008
D. Yang, Y. Gu, P. Tontiwachwuthikul**Wettability determination of the reservoir brine–reservoir rock system with dissolution of CO_2 at high pressures and elevated temperatures**
Energy Fuels, 22 (2008), pp. 504-509
CrossRefView Record in Scopus